# Supplementary Information

**High-performance reduced graphene oxide supercapacitors enabled by simple amino hydroquinone dimethylether**

Yang Luo [a], Haihui Lin[a], Yuxiao Chu [a], Jian Wang [a], Naxing Liu [a], Fu-Gang Zhao[*a], Lei Dong[*b], Yuegang Chen[*a] and Yongmiao Shen[*a]

[a]Department of Chemistry, Key Laboratory of Surface & Interface Science of Polymer Materials of Zhejiang Province, Zhejiang Sci-Tech University, 928 Second Street, Hangzhou 310018, China
[b]State Key Laboratory of Solidification Processing, Center of Advanced Lubrication and Seal Materials, School of Materials Science and Engineering, Northwestern Polytechnical University, Xi'an 710072, China
E-mail: donglei@nwpu.edu.cn (L. Dong), fgzhao@zstu.edu.cn (F.-G. Zhao), chenyg@zstu.edu.cn (Y. Chen), shenym@zstu.edu.cn (Y. Shen)

# Experimental section

## 1. Materials

Amino hydroquinone dimethylether (AHQDME) and Graphene oxide (GO) were purchased from Aladdin company. All other chemicals were used as received, without any further purification.

## 2. Characterization

Elemental analysis on carbon (C), hydrogen (H) and nitrogen (N) contents was carried out with an Elementar vario EL III elemental analyzer. Fourier transform infrared spectra (FT-IR) were recorded on a Nicolet Avatar-360 Fourier transform infrared spectrophotometer using a potassium bromide pellet. X-ray photoelectron spectroscopy (XPS) was conducted on a PHI-5000 VersaProbe spectrometer under 10-7 Pa using a monochromatic Al Kα X-ray source operating at 100 W. Raman spectra were performed on a Renishaw inVia Reflex micro-Raman spectrometer using a 100-fold objective lens and crystal laser excitation at 514.5 nm with a power of 0.1 mW. Atomic force microscopy (AFM) images were acquired under ambient conditions on a Veeco instrument Nanoscope IIIa Multimode apparatus operating in a non-contact mode with a silicon tip and cantilever operating at a frequency of 325 kHz and a scanning speed of 1 Hz. Samples were prepared by placing a drop of their dilute aqueous dispersion on a fresh mica substrate and dried in avacuum oven at room temperature. Field-emission scanning electron microscope (FESEM) was performed a Hitachi S-4800 operating at 3 kV. Transmission electron microscopy (TEM) and energy dispersive X-ray spectrometry (EDS) were performed on a FEI Tecnai G2 F20 S-TWIN electron

microscope operating at an accelerating voltage of 200 kV. Samples were prepared by placing a drop of their dilute chloroform dispersion on a holey-carbon-coated copper grid and dried in a vacuum oven overnight at room temperature. All the electrochemical tests were performed on a CHI660e electrochemical workstation at room temperature.

**3. Synthesis of rGO materials**

80 mL GO solution (0.5 mg $mL^{-1}$) was transferred into a 100 mL Teflon-lined stainless steel autoclave and heated at 140 ℃ for 24 h, and then naturally cooled to room temperature. During post-processing, the reaction mixtures were filtered over a 0.22 μm PTFE membrane, and the filter cakes were thoroughly washed by ethanol (500 mL×3), N,N-dimethylformamide (500 mL×3) and deionized water (500 mL×3), respectively, for removing any impurities. After being dried in a vacuum oven at 80 ℃ for 24h, the products were afforded.

**4. Synthesis of rGO-AHQDME heterojunction materials**

The rGO-AHQDME composite was obtained by a simple one-step hydrothermal method. The rGO-AHQDME composite was obtained by a simple one-step hydrothermal method. In detail, 80 mL GO solution (0.5 mg $mL^{-1}$) was firstly mixed with AHQDME ($W_{GO}$: $W_{AHQDME}$ =1:1) and stirred for 1 h at room temperature. And then, the mixture suffered from a sonication treatment for 0.5 h (40 KHz, 700W), affording homogeneous GO-AHQDME hybrid solutions. Then, the brown solution was transferred into a 100 mL Teflon-lined stainless steel autoclave and heated at 140 ℃ for 24 h, and then naturally cooled to room temperature. During post-processing, the reaction mixtures were filtered over a 0.22 μm PTFE membrane, and the filter cakes were thoroughly washed by ethanol (500 mL×3), N,N-dimethylformamide (500

mL×3) and deionized water (500 mL×3), respectively, for removing any impurities. After being dried in a vacuum oven at 80 ℃ for 24h, the products were afforded.

**Calculation details for the functionalization degree of rGO-AHQDME sample using EA data:**

It is widely accepted that EA provides much more real and accurate element content in comparison with other analysis methods, such energy dispersive spectrometer, X-ray photoelectron spectroscopy, etc.

It is detected that the sample contains C element of 67.60% and H of 3.70%, N of 5.70% and O of 23.00%, respectively. Because pure reduced graphene oxide does not contain N element, N element in the sample only stems from amino groups in functionalized graphene in the case that amino-hydroquinone-dimethylether (AHQDME) residues are thoroughly washed away. In this end, the N mass/molar amounts are 5.7g/0.4 mol for 100 g sample according to N content of 5.70%; the loading mass/molar amounts of AHQDME functionalities are 62.4g/0.4 mol.

Furthermore, according to the molecular formulas AHQDME, it can be readily calculated the C mass/molar amounts are 38.4 g/3.2 mol of AHQDME functionalities. By easy subtracting, the C mass/molar contributed from graphene scaffolds are 29.2 g/2.4 mol. The functionalization degrees (per 100 mol carbon atom of graphene containing x mol functional species) for rGO-AHQDME are 17.

# Electrochemical Measurements

**1. Work electrode fabrication:**

To a 10 mL vial, 0.0244 g sample as active materials, 0.0486 g 10 wt% PVDF/NMP (PVDF: polyvinylidene fluoride; NMP: N-methyl pyrrolidone) solution as binders, 0.0032 g Super-P powders as the conducting agents and ~3 mL ethanol solvent were added, respectively. Thereafter, the mixtures were stopped stirring until the system appeared sticky paste. And then the pasty slurries were uniformly coated on 1×1 $cm^2$ carbon clothes as the flexible current collectors using a Chinese brush pen. Subsequently, the as-prepared electrodes were dried overnight under vacuo at 80 ℃. The active materials in one single electrode were finely tuned to be around 1~2 mg and accurately weighed for the following capacitance calculations.

**2. Measurement and calculation methods:**

All the electrochemical tests were performed on a CHI660e electrochemical workstation at room temperature.

**In a three-electrode system:**

**In aqueous electrolyte:**

1.0 M aqueous $H_2SO_4$ solution was used as an electrolyte, a platinum foil (2×1 $cm^2$) and an Ag/AgCl saturated by KCl solution were used as the counter and reference electrodes, respectively. The electrochemical capacitive performances of the rGO-AHQDME samples were evaluated by cyclic voltammetry (CV), galvanometric charge/discharge curves (GCD), and electrochemical impedance spectroscopy (EIS) over a frequency range of 0.01 Hz to 100 kHz. CVs were carried out in a potential range of -0.2~ 0.8 V (v.s. Ag/AgCl) at varied scan rates from 20 to 200 mV $s^{-1}$. GCDs were carried out in a potential range of-0.2~ 0.8 V (v.s. Ag/AgCl) at varied current densities from 1.0 to 20.0 A $g^{-1}$.

**In organic electrolyte：**

1.0 M $EMIMBF_4$/AN solution was used as an electrolyte, a platinum foil (2×1

$cm^2$) and an Ag/AgCl saturated by KCl solution were used as the counter and reference electrodes, respectively. The electrochemical capacitive performances of the rGO-AHQDME samples were evaluated by cyclic voltammetry (CV), galvanometric charge/discharge curves (GCD), and electrochemical impedance spectroscopy (EIS) over a frequency range of 0.01 Hz to 100 kHz. CVs were carried out in a potential range of -1.6~ 0.8 V (v.s. Ag/AgCl) at varied scan rates from 10 to 100 mV $s^{-1}$. GCDs were carried out in a potential range of-1.6~ 0.8 V (v.s. Ag/AgCl) at varied current densities from 2.0 to 5.0 A $g^{-1}$.

**Calculations of capacitive characteristics:**

The gravimetric specific capacitance ($C_s$) derived from galvanostatic discharge curves was calculated based on the following equation:

$$C_s = I \times \Delta t/(m \times \Delta V)$$

Where I (A) was the constant discharge current, Δt (s) was the discharging time, m (g) was the mass of the active materials and ΔV (V) represented voltage drop during the discharging process.

**In a symmetric two-electrode cell setup:**

The pasty slurries were uniformly coated on round carbon paper with a diameter of 16 mm as the electrode. Subsequently, the as-prepared electrodes were dried overnight under vacuum at 80 ℃. The total mass (Mt) of the electrode material was calculated by subtraction method. All specific capacitance were calculated based on the neat mass of the active material in the electrode material, which was calculated by 0.75×Mt. Before assembling two-electrode cell, the electrolyte solution was prepared using a mixture of acetonitrile (AN) and $EMIMBF_4$ (1:1, mass ratio). Nylon (PA) membrane was used as an electron separator. The assembly process was carried out in an argon-filled glovebox (LABmaster).

The gravimetric specific capacitance ($C_s$) of the electrode material in the whole device was calculated from the galvanometric discharge curve based on the following formulas:

$$C_s = 4\frac{I \cdot \Delta t}{m \cdot \Delta V}$$

where I (A) is the constant discharge current, Δt is the discharging time, m is the total mass of the active material in both electrodes for two-electrode cells, ΔV represents the potential window. The gravimetric and volumetric energy densities ($E_W$) in two-electrode device were calculated using the following formulas:

$$E_W = 0.125C_s \times (\Delta V)^2/3.6$$

Where $C_s$ (F $g^{-1}$) was the specific capacitance of the electrode material in the whole device, ΔV (V) represented voltage drop during the discharging process.

The gravimetric power densities ($P_W$) were calculated using the following formulas:

$$P_W = 3600\frac{E_W}{\Delta t}$$

Where $E_W$ (Wh $kg^{-1}$) was the energy density of the whole device, Δt (s) was the discharging time.

**Electrical conductivity tests and calculations**:

The sheet resistances of rGO-AHQDME sample was measured on a 280SI four-point probe system (Four Dimensions Inc., USA). The sheet resistance (Rs) data for the sample was obtained by averaging three sheet resistance values collected from different testing positions. The membrane/film thicknesses (*h*) of the corresponding samples were tested by a CHY-U Sumspring gauge. The electrical conductivity (σ) of membrane/film samples can be derived from the formula:

$\delta = 1/(R_s \times h)$

The parameters of rGO-AHQDME films were listed in **Table S1** as following: **Table S1**. The measured parameters of sheet resistance (*Rs*) and thickness (*h*), and the calculated electrical conductivity (σ) for rGO-AHQDME films.

**Table S1. The measured parameters of sheet resistance (Rs) and thickness (h), and the calculated electrical conductivity (σ) for rGO-AHQDME heterojunction films.**

| Product | FD | Samples | $R_s$ (Ω/□) | h (nm) | σ (S/cm) | Average σ (S/cm) |
|---|---|---|---|---|---|---|
| rGO-AHQDME | 17 | Sample1 | 12165 | 127 | 6.5 | 6.5 |
| | | Sample2 | 11898 | 130 | 6.5 | |
| | | Sample3 | 11746 | 132 | 6.4 | |

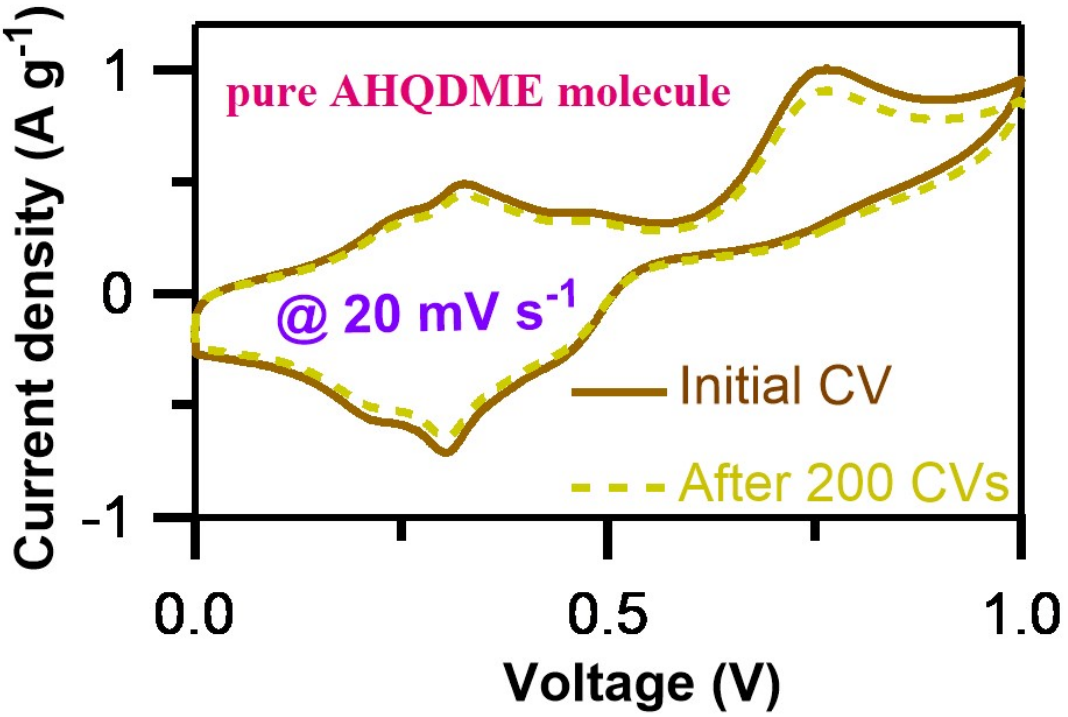


**Fig. S1.** CV curves of AHQDME in aqueous $H_2SO_4$ electrolyte in prototype

three-electrode cell.

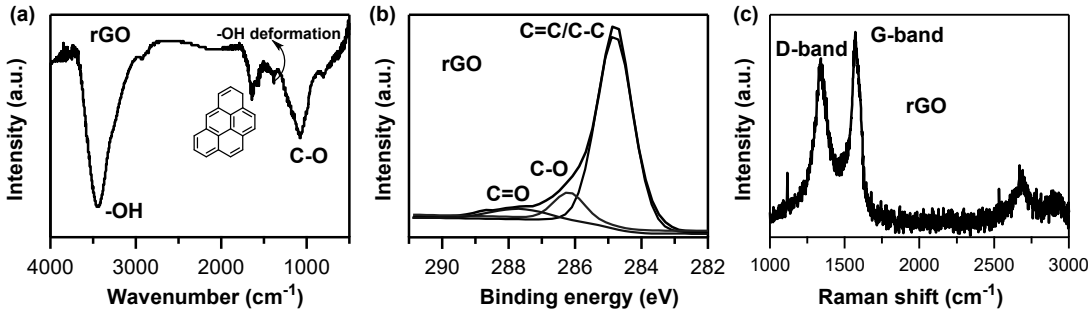


**Fig. S2.** (a) FT-IR, (b) C1s XPS, (c) Raman spectra of reduced graphene oxide (rGO).

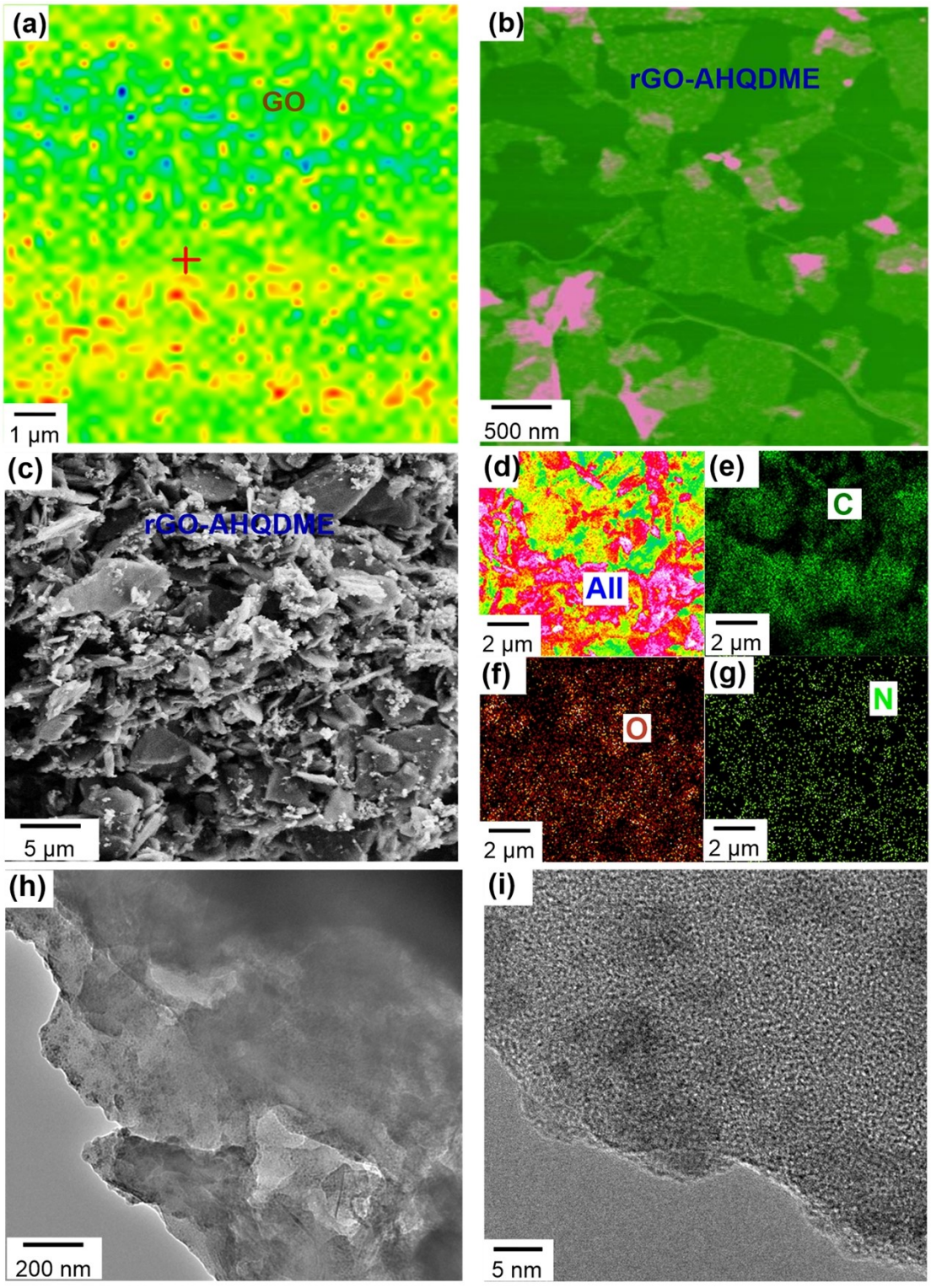


**Fig. S3.** (a) Raman mapping images of GO. (b) AFM images and (c) FESEM spectra of rGO-AHQDME. (d–g) EDS mappings of rGO-AHQDME for all elements tested, C, O, and N. (h) and (i) TEM images of rGO-AHQDME.

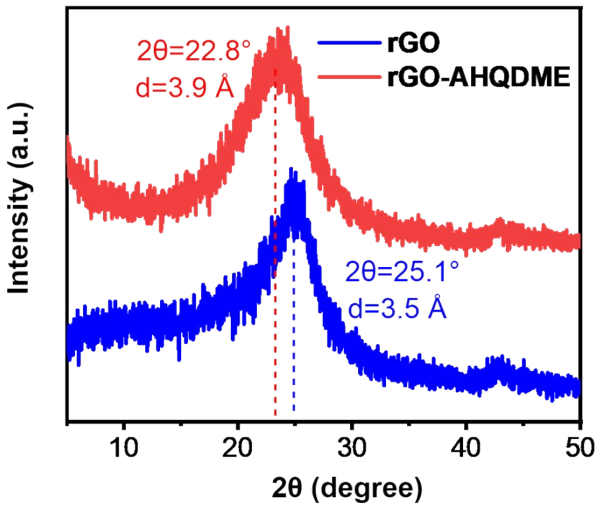


**Fig. S4.** X-ray diffraction pattern of rGO and rGO-AHQDME heterojunction material.

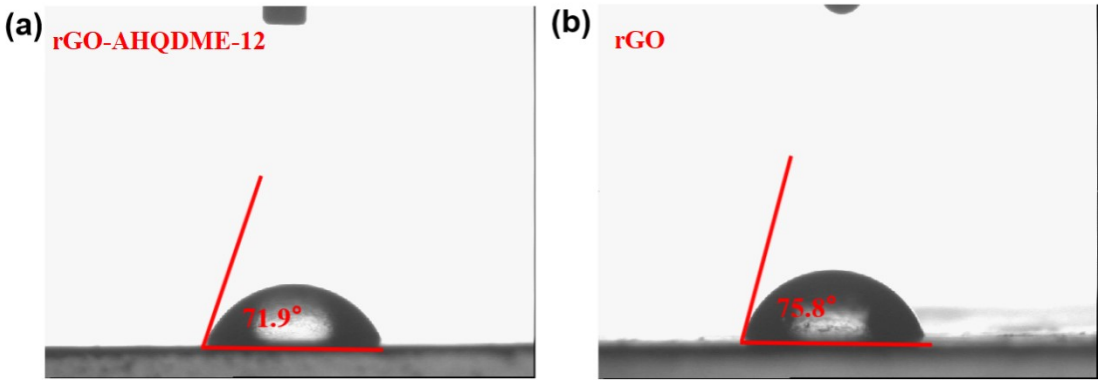


**Fig. S5.** Contact angle image of (a) rGO-AHQDME-12 (b) rGO films.

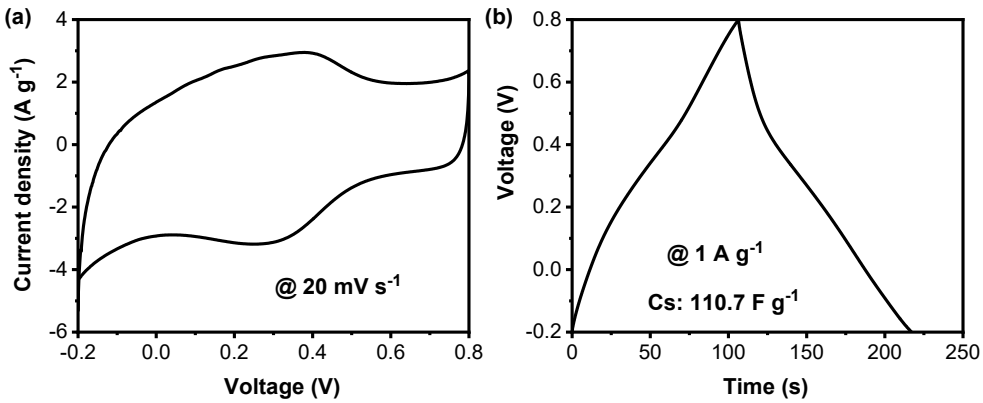


**Fig. S6.** (a) CV, (b) GCD curves of rGO electrode in aqueous three-electrode cell.

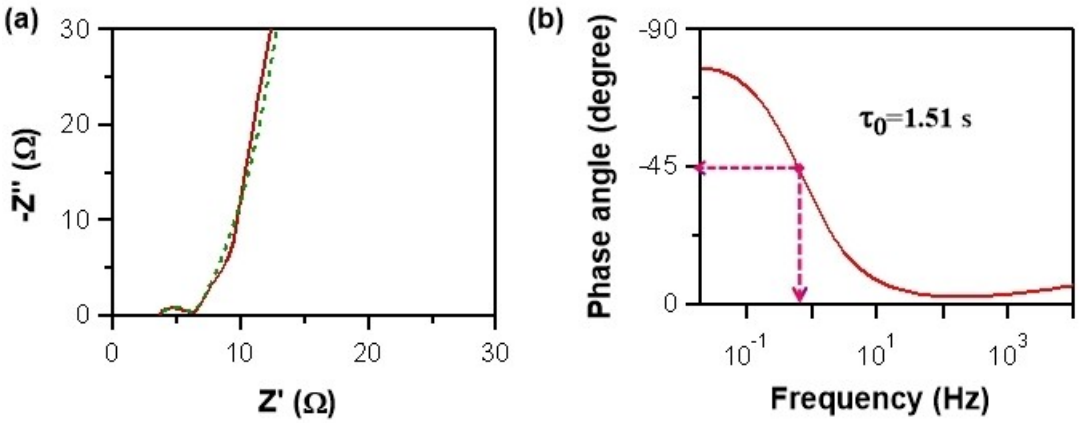


**Fig. S7.** (a) EIS-Nyquist and (b) Bode plots of rGO-AHQDME in organic electrolyte in the prototype three-electrode cell.

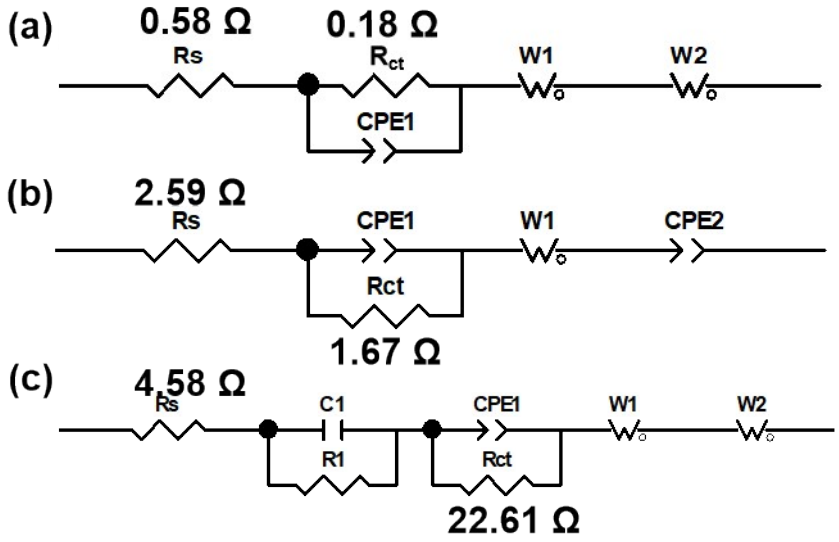


**Fig. S8.** The simulated equivalent circuit by Z-view software of (a) rGO-AHQDME in aqueous electrolyte in prototype three-electrode cell, (b) rGO-AHQDME in organic electrolyte in prototype three-electrode cell, (c) rGO-AHQDME//rGO-AHQDME in organic electrolyte with symmetric two-electrode coin device. The equivalent circuit consists of the following parts: Rs, Rct, W, Cdl and CPE, where Rct represents the charge transfer resistance, Rs represents the bulk solution resistance, W represents the Warburg impedance of diffusive resistance, Cdl means the double-layer capacitance and CPE means the constant phase element.

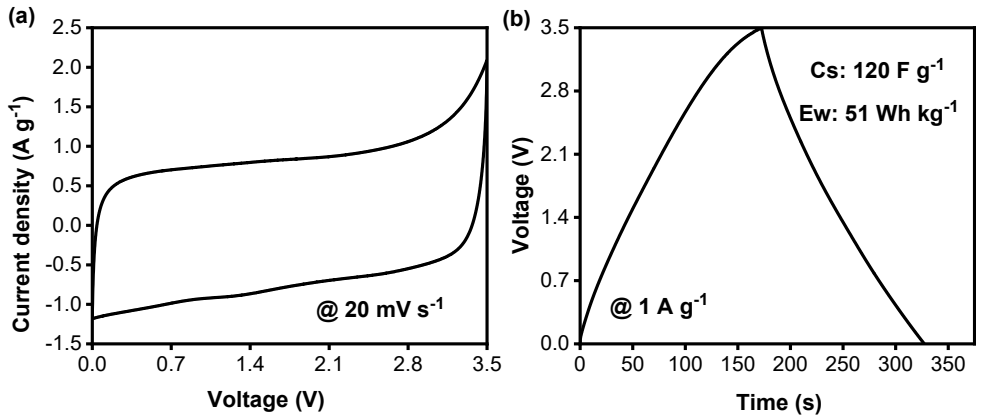


**Fig. S9.** (a) CV, (b) GCD curves of rGO//rGO symmetrical two-electrode cell.

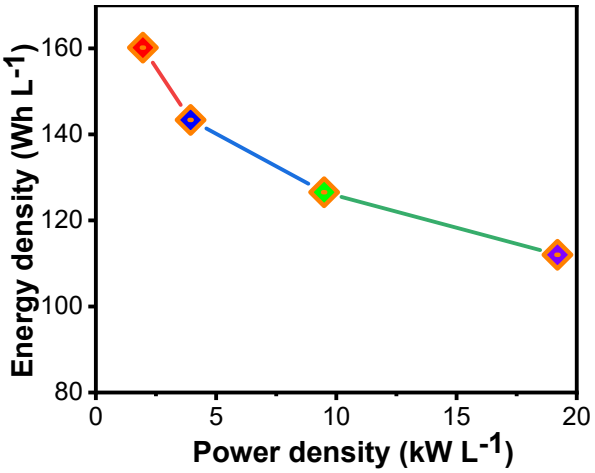


**Fig. S10.** Ragone plot in volumetric metric.

**Table S2.** Comparisons of energy-storage performances of the prepared rGO-AHQDME//rGO-AHQDME symmetric two-electrode coin in this work with other recently reported materials.

| Electrode materials | Electrolytes (Voltage/V) | $C_s$ (F $g^{-1}$) | $E_w$ (Wh $kg^{-1}$) | Capacitance retention/cycling times |
|---|---|---|---|---|
| This work | $EMIMBF_4$/ AN (3.5 V) | 338 | 143 | 91%/10000 |
| MWNTs[1] | $LiClO_4$ / AND-AN-DMC (2 V) | 136.6 | 71.1 | 84%/10000 |
| NAC950[2] | $SBPBF_4$/PC (2.7V) | 134 | 35.7 | 84.3%/10000 |
| AC/MXene-2:1[3] | $Et_4NBF_4$/AN (2 V) | 126 | 17.5 | 92.4%/100000 |
| Zn-BHS[4] | DMF/Zn-TFMS (1.8 V) | 112 | 58.1 | 84%/5000 |

| | | | | |
|---|---|---|---|---|
| FCNS[5] | IL-AN/Zn($CF_3SO_3$)$_2$ (1.8 V) | 226 | 10.86 | 97.8%/ 60 000 |
| Zn-CMP-S[6] | AN/ TEA $BF_4$ (2.7 V) | 136 | 34 | 82%%/10000 |
| GNPC-0.75[7] | PC/EMIM$BF_4$-TEA$BF_4$ (3 V) | 397 | 124.1 | 98 %/60000 |
| ACF[8] | AN/ TEA$BF_4$ (2.7 V) | 112 | 29.50 | 87 %/10000 |
| CP-Cr[9] | DMSO /TEA$BF_4$ (3 V) | 48.7 | 60.8 | 77 %/5000 |
| SHS@SC[10] | PC/TEA$BF_4$ (1.6 V) | 29.6 | 9.67 | 90.9 %/3000 |

## References


1 C. Song, J. Yun, H. Lee, H. Park, Y. R. Jeong, G. Lee, M. S. Kim and J. S. Ha, *Adv. Funct. Mater.*, 2019, **29**, 1901996.

2 Z.-F. Wang, Z. Yi, S.-C. Yu, Y.-F. Fan, J. Li, L. Xie, S.-C. Zhang, F. Su and C.-M. Chen, *ACS Appl. Mater. Interfaces*, 2022, **14**, 24497-24508.

3 L. Yu, L. Hu, B. Anasori, Y.-T. Liu, Q. Zhu, P. Zhang, Y. Gogotsi and B. Xu, *ACS Energy Lett.*, 2018, **3**, 1597-1603.

4 X. Qiu, N. Wang, Z. Wang, F. Wang and Y. Wang, *Angew. Chem. Int. Ed.*, 2021, **60**, 9610-9617.

5 H. Zhou, C. Liu, J.-C. Wu, M. Liu, D. Zhang, H. Song, X. Zhang, H. Gao, J. Yang and D. Chen, *J. Mater. Chem. A*, 2019, **7**, 9708-9715.

6 N. Talreja, S. Jung, L. T. H. Yen and T. Kim, *Chem. Eng. J.*, 2020, **379**, 122332.

7 X. Shi, S. Zhang, X. Chen, T. Tang and E. Mijowska, *Carbon*, 2020, **157**, 55-63.

8 M. Vijayakumar, R. Santhosh, J. Adduru, T. N. Rao and M. Karthik, *Carbon*, 2018, **140**, 465-476.

9 S. Acharya, S. Sahoo, S. Sonal, J. H. Lee, B. K. Mishra and G. C. Nayak, *Composites, Part B*, 2020, **193**, 107913.

10 J. Shang, Q. Huang, L. Wang, Y. Yang, P. Li and Z. Zheng, *Adv. Mater.*, 2020, **32**, 1907088.